Grey Wolf Optimization based hybrid SVM for Finger Vein Recognition

Manpreet Singh[1]
[1]Research Scholar, University of Waterloo, Waterloo, Canada

***Abstract* - Finger Vein Recognition (FVR) technique has emerged to be the most anticipated and novelist biometric approach due to its low device constraint, consistency, internal characteristic, aliveness detection, low forgery risk, and enable a very high level of security. The accuracy of the personal recognition system is the most severe issue to reflect on. To address this problem, Swarm intelligence Meta-heuristic optimization algorithm has been employed to improve classification. In this research work, an efficient finger vein recognition framework based on GWO-SVM approach has been proposed considering the above-mentioned challenges. Image acquisition, Image Pre-processing, Feature Extraction and Matching/Classification (Imposter or Genuine) are four prominent steps implemented in this work. Finger vein images are acquired from two public finger vein datasets and are pre-processed to extract robust ROI (Region of Interest). Hybrid feature extraction technique integrating Local Phase Quantization (LPQ), which is invariant to blur and deformation, and Local Directional Pattern (LDP), which is robust to random noise and illumination variations, is implemented to extract robust and accurate features. Furthermore, these selected features are provided as input to a Support Vector Machine (SVM), which implements Radial basis kernel function. The pair (C, σ) is required to be optimized to augment the accuracy of SVM. Thus, GWO is used as an efficient tuning algorithm for obtaining the best SVM parameters which significantly improves its classification accuracy and the proposed GWO-SVM approach is implemented. The performance of the proposed framework is evaluated on the two finger vein datasets: HKPU and FV-USM.**

Keywords: Biometric recognition, Finger Vein, Hybrid Feature extraction, Support vector machine, Grey Wolf Optimization

I. INTRODUCTION

A. Biometric recognition

Personal identification technology is used in a wide-ranging system for tasks such as area access control and logins for PCs and e-commerce systems. Biometric techniques which comprise fingerprint, retina, iris, and face recognition for recognizing individuals, are drawing attention since Conventional identification mechanisms such as PINs, passwords, keys etc. carry potentially the high risk of being repudiated, stolen or lost and hence, insufficient to provide reliable and secure identity verification [1]. Likewise, it gives rise to an efficient identity recognition technique against biologically dependent impersonation. The standard hedges against identity fraud such as passwords and personal identifying numbers (PINs) are known to be less accurate.

As there is an increased demand of user-friendly personal identification, the biometric authentication systems have become a blooming research area. Biometrics is defined as a physical or behavioral trait that is uniquely associated to a person. Various common examples of biometrics include finger, voice, face, iris recognition, etc. Identifying human face was the first biometric method to provide security. Biometric systems are being already deployed in various sectors such as corporate sector, banking, railway systems and education sector as well to attain high levels of security.

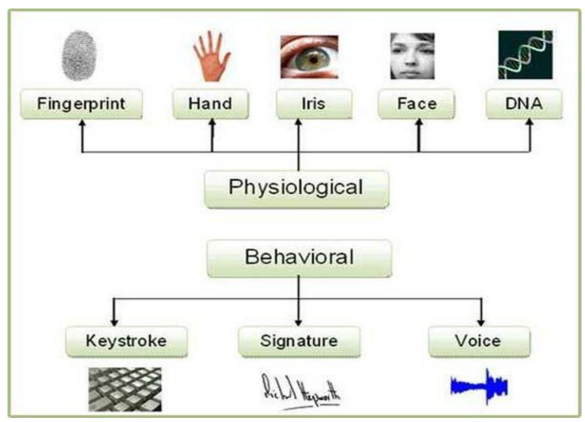

Figure 1. Categories of Biometrics [1]

B. Finger Vein Recognition (FVR)

Today, with the rapid growth in the field of computer and network technology, the identity verification is a critical key problem. Thus, the requirement for a better and more reliable approach for identity authentication becomes more significant. Conventional identification mechanisms such as PINs, passwords, keys etc. carry potentially the high risk of being repudiated, stolen or lost and hence, insufficient to provide reliable and secure identity verification. Subsequently, it gives rise to an effective technique of identity recognition against digital impersonation based on biological features. Biometric recognition utilizes inherent physical features and behavioral characteristics of an individual. Examples of physiological features are face, fingerprint, iris, vein, etc. Few examples of behavioral characteristics are like handwriting, voice, signature, etc. [2].

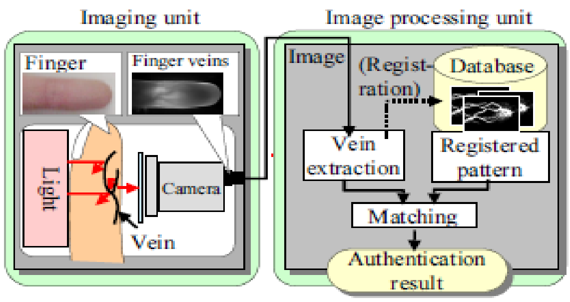

Figure 2. Flow of finger-vein recognition system [1]

However, these conventional biometric techniques have their limitations regarding performance, accuracy, consistency and convenience. Hand-based biometrics generally comprise fingerprint recognition, finger knuckle print recognition, and palm print recognition. However, all these traits are unique to human bodies and are thus more vulnerable to forgery.

Amongst these biometric techniques, finger vein recognition technique has become the most preferred biometric method due to its low device constraint, aliveness detection, low forgery risk, stability, and high anti counterfeit. As an intrinsic physical characteristic, finger vein possesses higher security over other extrinsic biometric traits (*such as* face and fingerprint) owing to trouble in replicate or steal the trait. The non-invasive and contactless capture of finger-veins are more appropriate and sterile for the user, and thus, it is more suitable. Moreover, another significant advantage of finger vein is the aliveness detection, which means only the vein in a living finger can be acquired, hence, it cannot be tampered by artificial veins.

Compared with other biometric characteristics, the finger-vein exhibits unique advantages such as [2]:

a) **Resistant to criminal tempering:** As veins are internal to the human body, there is low threat to forgery.
b) **High accuracy:** For the False Rejection rate (FRR), the recognition accuracy is relatively less than 0.01 % and 0% for failure to enrol.
c) **Unique and constant:** The vein patterns are distinct and remains unchanged even among the identical twins.
d) **Contactless:** Once the finger vein images are captured via the near-infrared light, it permits contactless imaging that ensures complete suitability and hygiene for the individual practice.
e) **Ease of Feature extraction:** The vein patterns are immutable and clearly captured due to which vein images are acquired with low resolution.
f) **Fast authentication speed:** Authentication devices consume much less time as fingers or palm has to merely hover over the device and authenticate itself.

The main applications of finger vein biometrics include ATM, Internet Banking, physical access control, cellular phone, national ID card, driver's license, passport control, corpse identification, criminal investigation, Airport Security, Time and Attendance, Law Enforcement etc.

The rest of the paper is structured as follows: Literature survey is introduced in Section II. Section III presents methods and material for finger vein recognition and Section IV introduces the current method. Section V provides experimental results and discussions. Finally, conclusion of this paper is reported in section VI.

II. LITERATURE SURVEY

In this section, various finger vein feature extraction and recognition methods reported in the literature are extensively reviewed for their effectiveness and limitations respectively. Different finger vein feature extraction and classification techniques have been developed in the recent past. Although the performance of finger vein recognition has been promoted by the reviewed methods in recent years, dramatic performance improvement has not yet been achieved. A concise review of literature is specified below:

Bakhtiar Affendi Rosdi et.al [19] introduced a new classifier called fuzzy based k-nearest centroid neighbor (FkNCN). The k-nearest centroid neighbors are obtained and to assign the test image to a particular class, a fuzzy membership function is used. This proposed method exhibits far more better performance than the fuzzy-based k-nearest neighbor classifier and k- nearest centroid neighbor classifier.

Shazeeda et.al [24] proposed Mutual Sparse Representation classification (MSRC), a very effective and efficient method for finger vein recognition. A new decision rule is employed by MSRC to classify the test samples, thus improving the recognition rate of SRC to a great extent. Using this approach of a new decision rule, the classification of the test sample is dependent on the nearest sparse neighbor.

Xiaoming Xi et.al [20] used a discriminative binary codes (DBC) learning for recognition. An optimization problem is formed from the graphs and the distance is maximized between templates. Therefore, the maximum amount of information is provided by the templates. The binary templates obtained are further used for training instances by providing supervised information.

In this paper **Yu Lu et.al [7]** proposed a new local descriptor called pyramid histogram of double competitive pattern (PHDCP). Due to finger vein system's abundant features and fine network, finger vein is a reliable and secure biometric. Nonetheless, the existing local descriptors can not represent these features due to its limitations. This paper proposed PHDCP to efficiently use these features in finger vein pictures. Gabor filters are used to obtain a set of filtered images with rich orientation. At last, the hierarchical features are obtained from the image by the pyramid histogram extraction method.

Rig Das et.al [8] states that although, the current state-of-the-arts techniques obtain an extremely good high performance, but they are highly dependent upon the quality of the image. A convolutional neural network is proposed to make a finger vein recognition system and the performance of the network is evaluated on the four publicly available databases. To obtain high performance, a deep learning method is proposed for finger vein recognition.

III. MATERIALS & METHODS

In this paper, a Finger Vein Recognition framework based on the hybrid feature extraction technique is proposed that extracts features using the combination of Local Phase Quantization (LPQ) and Local Directional Pattern (LDP) techniques. The resultant feature vector is applied as an input to the SVM to perform classification of finger vein images as either imposter or genuine. The methodology is described in detail as follows:

A. Local Phase Quantization (LPQ)

LPQ is a robust and efficient frequency domain-based blur-invariant feature extraction technique that extracts the local phase information of the image using Short Term Fourier Transform (STFT) - 2-D discrete Fourier transform, over a rectangular region. LPQ operator distributes the label image into equal-sized non-overlapping rectangular sections. Each sub region of the label image is computed independently to extract relevant and useful local information. It is invariant to optical image blur and deformation, uniform illumination variations but still quite descriptive and discriminative. LPQ applies the STFT algorithm to compute the local phase spectrum of an N*N image. A 256-dimensional feature vector composed as a histogram is obtained for each image and these LPQ features are used in classification.

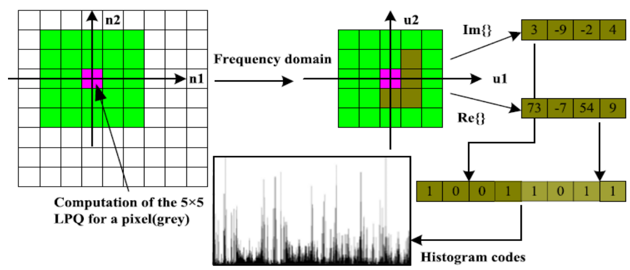

Figure 3. LPQ computation procedure [3]

B. Local Directional Pattern (LDP)

Another efficient local feature-based descriptor, Local Directional Pattern, generates LDP features on the basis of well-known Kirsch kernels. The edge response values against each pixel position is computed in all 8-directions in order to generate the LDP feature. An 8-bit binary code is allocated to each pixel. It compares the edge response values in eight distinct directions to evaluate a pattern. It is insensitive to existing noise, illumination fluctuations, aging effects etc. An accumulated 186-dimensional LDP feature vector is obtained for each image.

$$\underset{\text{East } M_0}{\begin{bmatrix} -3 & -3 & 5 \\ -3 & 0 & 5 \\ -3 & -3 & 5 \end{bmatrix}} \quad \underset{\text{North East } M_1}{\begin{bmatrix} -3 & 5 & 5 \\ -3 & 0 & 5 \\ -3 & -3 & -3 \end{bmatrix}} \quad \underset{\text{North } M_2}{\begin{bmatrix} 5 & 5 & 5 \\ -3 & 0 & -3 \\ -3 & -3 & -3 \end{bmatrix}} \quad \underset{\text{North West } M_3}{\begin{bmatrix} 5 & 5 & -3 \\ 5 & 0 & -3 \\ -3 & -3 & -3 \end{bmatrix}}$$

$$\underset{\text{West } M_4}{\begin{bmatrix} 5 & -3 & -3 \\ 5 & 0 & -3 \\ 5 & -3 & -3 \end{bmatrix}} \quad \underset{\text{South West } M_5}{\begin{bmatrix} -3 & -3 & -3 \\ 5 & 0 & -3 \\ 5 & 5 & -3 \end{bmatrix}} \quad \underset{\text{South } M_6}{\begin{bmatrix} -3 & -3 & -3 \\ -3 & 0 & -3 \\ 5 & 5 & 5 \end{bmatrix}} \quad \underset{\text{South East } M_7}{\begin{bmatrix} -3 & -3 & -3 \\ -3 & 0 & 5 \\ -3 & 5 & 5 \end{bmatrix}}$$

Figure 4. Kirsch edge response masks in eight directions [4].

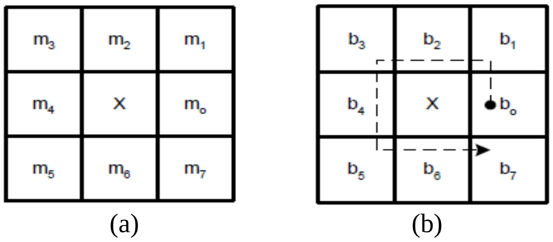

Figure 5. (a) Eight directional edge response positions. (b) LDP binary bit positions [4].

Eight edge response values $m_0, m_1 \dots m_7$ are obtained by applying these eight masks, each signifying the edge in its respective direction. The presence of corner, junction or edge show high response values in particular directions because the response values are not equally important in all directions. The k most significant directions for a pixel must be obtained in order to produce the LDP. The top-k directional bit responses of the 8-bit LDP pattern, b_i, are set as 1. The remaining (8 − k) bits are set as 0.

$$LDP_k = \sum_{i=0}^{7} b_i\,(m_i - m_k) \times 2^i,\ b_i(a) = \begin{cases} 1, & a \geq 0, \\ 0, & a < 0, \end{cases} \quad (1)$$

where m_k is the k-th most prominent directional edge response.

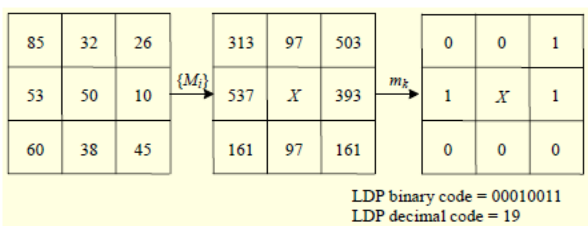

Figure 6. LDP code with k =3 [4].

C. *Support Vector Machines (SVM)*

In this research, SVM performs binary classification by developing a high dimensional optimal separating hyperplane. Let $S = \{(x_1, y_1), (x_2, y_2), \dots, (x_n, y_n)\}$ is a training dataset with n samples, where x_i is a n-dimensional feature vector and $y_i \in -1, 1$ is the class label (classes $C1$ and $C2$). Geometrically, obtaining an optimal hyperplane with the greatest margin requires to elucidate the optimization problem, as shown in Eqs. (12) and (13).

$$maximize\ \sum_{i=1}^{n} \alpha_i - \frac{1}{2}\sum_{i,j=1}^{n} \alpha_i \alpha_j\, y_i y_j . K(x_i, x_j) \quad (12)$$

$$Subject - to:\ \sum_{i=1}^{n} \alpha_i y_i\ , 0 \leq \alpha_i \leq C \quad (13)$$

where, α_i is the weight assigned to each training sample x_i. If $\alpha_i > 0$, x_i is called a support vector. C is a regulation parameter and k is a kernel function.

The resultant hybrid feature vector is fed as an input to SVM. SVM is used to classify the finger vein images in binary classes – IMPOSTER or GENUINE. Train set, Train class, sigma and smoothness parameter is provided as input to the "svmtrain" function 'C'. By default, sigma=0.5 and C = 1. Radial basis kernel function is implemented to map the input data points to a higher dimensional space. SVM is trained and tested using radial basis function kernel. SVM is used with a radial basis function (RBF) kernel having width σ which reflects the distribution/range of x-values of training data is given by:

$$K(x, y) = \exp\left(-\|x - y\|^2 / 2\sigma^2\right) \quad (14)$$

where, $K(x, y)$ is termed as the kernel function, which is referred to the dot product of two invariant x and y. The parameter C and the kernel parameter σ are required to train SVM classifier and these two parameters are required to be optimized using GWO algorithm for efficient results. The results of the typical-SVM are compared with the proposed hybrid GWO-SVM approach.

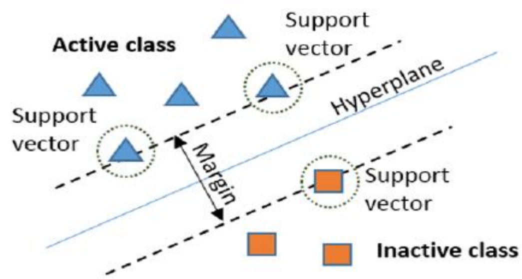

Figure 7. Maximum-margin hyperplane and margins for an SVM trained with samples from two classes [6].

D. *Grey Wolf Optimization (GWO) Algorithm*

A recent meta-heuristic approach (GWO), inspired by grey wolves, was proposed by Mirjalili et al. (2014) [5]. This new swarm intelligence algorithm works on the principle of imitating the hierarchical relationship and hunting mechanism of grey wolves in nature. Generally, grey wolves live in a group with a size of 5 to 12. The GWO algorithm primarily contains four units: social hierarchy, tracking/hunting, encircling, and attacking prey procedure. As for social hierarchy, grey wolves are essentially categorized into four varieties such as alpha (***α***), beta (***β***), delta (***δ***) and omega (***ω***) to simulate the wolf leadership hierarchy, as indicated in Fig. 8.

Alpha wolf is the main leader (decision-maker) and

Beta & Delta wolf assist Alpha wolf in decision-making or other activities. The hunting (optimization) is directed by three leading wolves with the maximum fitness (α, β and δ). The ω wolves follow them.

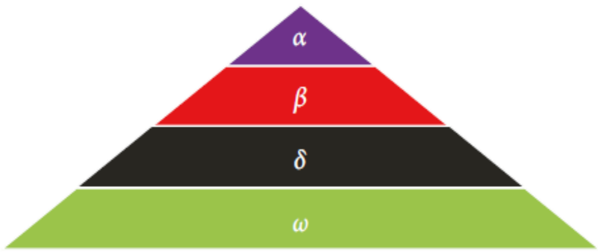

Figure 8. Leadership hierarchy of grey wolves [5]

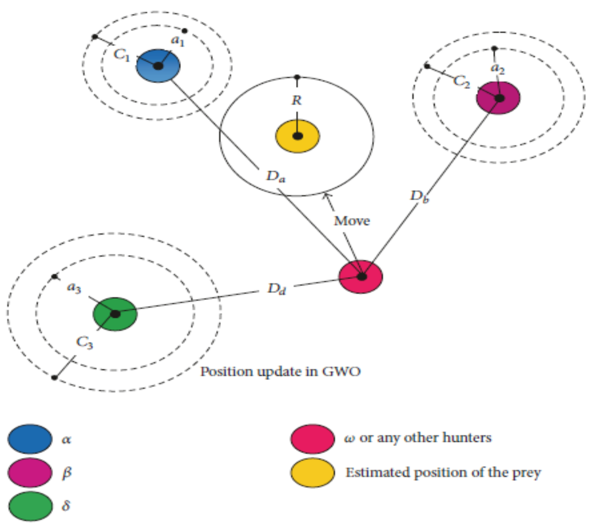

Figure 9. Position Update in GWO [5]

IV. Proposed Methodology

Finger vein recognition typically comprises four main phases: Image acquisition (finger vein datasets), Image pre-processing, Feature Extraction, Matching (Classification). *Feature Extraction and Matching* are the essential steps of finger vein recognition, which determines the recognition performance of the system to a large extent.

A. Image Acquisition:

Four widely used public finger vein datasets are used for image acquisition in order to evaluate and compare the performance of the proposed framework: HKPU [35], FV-USM [33], THU-FVDT2 [36] and SDU-MLA [34]. They contain both training and testing images of index and middle fingers of both hands for evaluation.

B. Pre-processing (Region of interest extraction):

The Finger vein image data sets (training and testing) are pre-processed using image enhancement, segmentation etc. as the original finger vein image is always low in contrast due to random noise, poor illumination and intensity variations. Therefore, image pre-processing is applied to resize or crop a finger vein image and to extract robust ROI (Region of Interest) for a more efficient finger vein feature extraction.

C. Hybrid LPQ-LDP Feature Extraction:

After pre-processing, the required features are extracted from the finger vein images using hybrid feature extraction technique integrating Local Phase Quantization (LPQ) and Local Directional Pattern (LDP) which is invariant to optical image blur, deformation, illumination variations, existing noise, misalignment etc. The relevant features are selected from the extracted features and stored as a feature vector.

1) LOCAL PHASE QUANTIZATION (LPQ)

Algorithm 1:
Step 1: For each pixel *x*, local phase coefficients are computed by applying STFT in the local neighborhood *Nx* as follows:

$$F(u,x) = \sum_{y \epsilon N_x} f(y)\omega_R(y-x)e^{-j2\pi u^T y} \qquad (6)$$

where $\omega_R(x)$ is a rectangular window function.

Step 2: The STFT is efficiently estimated for every image location $x \in \{x_1, x_2, \dots, x_N\}$ using solely 1-D convolutions in succession for the rows and columns.

Step 3: At four low frequency elements, the local Fourier coefficients are evaluated: $u_1 = [a,0]^T$, $u_2 = [0,a]^T$, $u_3 = [a,a]^T$, $u_4 = [a,-a]^T$ where a is a scalar that is necessarily small.
Step 4: For each pixel location, the following vector is obtained as an outcome:

$$F_x = [F(u_1,x), F(u_2,x), F(u_3,x), F(u_4,x)] \qquad (7)$$

Step 5: The phase information is scrutinized in the Fourier coefficients by observing the signs of the real and imaginary measures of each element in F_x. This is achieved by using a binary quantizer.

$$q_j = \begin{cases} 1, & g_j \geq 0 \\ 0, & otherwise \end{cases} \quad (8)$$

where g_j is the j-th element of the vector $F_x = [Re\{F_x\}, Im\{F_x\}]$.

Step 6: The resultant 8-bit binary coefficients g_j are denoted in the range of integer values (0-255) via binary coding:

$$f_{LPQ}(x) = \sum_{j=1}^{8} q_j\,(x) 2^{j-1} \quad (9)$$

where f_{LPQ} is the label image containing values which are the blur insensitive LPQ labels.

Step 7: Subsequently, these values are composed as a histogram, and described as a 256-dimensional feature vector.

2) LOCAL DIRECTIONAL PATTERN (LDP)

Algorithm 1:

Step 1: Kirsch masks, Mi computes the 8-directional edge response values $\{m_i\}$, *i*=0, 1,…,7 in eight different directions, for a given central pixel in the image.

Step 2: 8-edge response values $m_0, m_1 \ldots m_7$ are obtained by applying eight masks.

Step 3: In the 8-bit LDP pattern, the *k* most significant directions b_i, are set equal to 1. The residual (8 − k) bits are set equal to 0, as illustrated in the following equation:

$$LDP_k = \sum_{i=0}^{7} b_i\,(m_i - m_k) \times 2^i,\; b_i(a) = \begin{cases} 1, & a \geq 0, \\ 0, & a < 0, \end{cases} \quad (10)$$

where m_k is the *k*-th most prominent directional edge response.

Step 4: After extracting the local texture features using LDP, histogram is composed to label these features.

Step 5: The resultant LDP histogram is computed as the following equation:

$$H_{LDP_i} = \sum_{x,y} f(LDP_k(x,y), c_i) \quad (11)$$

Here, $f(a, c_i) = \begin{cases} 1, & a = c_i \\ 0, & otherwise \end{cases}$,

c_i is value of LDP code.

Finally, both LPQ and LDP are implemented for a robust feature extraction and the corresponding LPQ and LDP histograms are combined on the basis of mean values of the histogram, respectively, to obtain an enhanced histogram combining the features of both the techniques.

D. Grey Wolf Optimization Algorithm:

The three significant phases of hunting are applied to perform the optimization: searching, encircling the prey, and attacking towards prey. The hunting (optimization) is directed by three leading wolves with maximum fitness (α, β and δ). The ω wolves follow them.

1) Encircling prey:

The encircling prey actions can be mathematically demonstrated as the following equations:

$$X\,(t+1) = X_p(t) - A \cdot D, \quad (15)$$

where X_p is the location (position) of prey, A is the coefficient vector, and D is defined as

$$D = |C \cdot Xp(t) - X(t)|, \quad (16)$$

where C is the coefficient vector, X is the location of grey wolf, and *t* represents current iteration. The coefficient vectors, A and C, are determined by

$$A = 2a \cdot r_1 - a, \quad (17)$$

$$C = 2r_2, \quad (18)$$

where elements of *a* are reduced from 2 to 0 in a linear manner, in the sequence of iterations and r_1 , r_2 are random vectors in [0, 1].

2) Hunting:

In the course of hunting, the first three prominent solutions (α, β, and δ) attained are saved and induce other search agents (including ω) to adjust their positions conferring to the position of the best search agents. Basically, the leaders are pointing the ω wolves towards an optimal position. Eqs. (19–21) are being applied to modify the grey wolves' positions:

$$D_\alpha = |C_1 \cdot X_\alpha - X|,\; D_\beta = |C_2 \cdot X_\beta - X|,\; D_\delta = |C_3 \cdot X_\delta - X| \quad (19)$$

$$X_1 = |X_\alpha - A_1 \cdot D_\alpha|,\quad X_2 = |X_\beta - A_2 \cdot D_\beta|,\; X_3 = |X_\delta - A_3 \cdot D_\delta| \quad (20)$$

$$X(t+1) = \frac{X_1 + X_2 + X_3}{3} \qquad (21)$$

GWO overcomes the possibility of local optimal solutions, convergence rate and has greater exploration and shared information about the search space.

E. GWO Flowchart:

GWO can be summarized by steps shown in **Algorithm 1**.

1: Initialize the grey wolf population

$$X_i, (i = 1,2 \dots, n)$$

2: Initialize coefficient vectors, *A* and *C*, parameter *a*,

3: Compute the fitness value of each search agent, as:

X_α= the best search agent,

X_β= the second-*best* search agent,

X_δ= the third best search agent

4: set t: = 0

5: **while** *t* < *Maxnumberofiterations* **do**

6: **for** <each agent> **do**

7: Update the position of the current search agent by equations (19-21).

8: **end for**

9: Update *a, A, and C*

10: Calculate the fitness of all search agents

11: Update X_α, X_β, and X_δ

12: *t* = *t* + 1

13: **end while**

14: return $\boldsymbol{X_\alpha}$, the best solution produced.

Algorithm 1: Grey Wolf Optimization

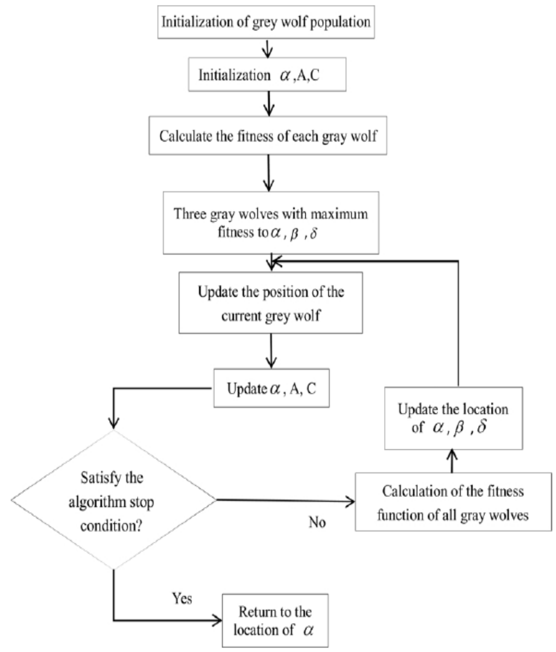

Figure 10. GWO Algorithm Flowchart

F. Proposed GWO-SVM Hybrid Approach

The proposed approach aims to automatically estimate the optimal values of the SVM parameters and hence, optimizing the SVM classification accuracy. The input to the GWO-SVM are combined feature vectors and their corresponding classes, GWO initialized parameters, whereas the output is the optimal SVMs parameters. SVM accuracy highly depends on the soft margin parameter (C) and kernel function parameter, sigma (σ). Thus, the pair (C, σ) is required to be optimized by Grey Wolf Optimization to augment the accuracy of SVM. After extracting the features for training data, the parameter values (C, σ) of SVM are dynamically optimized by GWO for finger vein recognition. After that, combined feature vectors are applied as an input to GWO-SVM classifier for verification task with the obtained optimal parameter values.

Steps of GWO-SVM are as follows: Firstly, the parameter optimization job is executed through the GWO algorithm. Secondly, the SVM optimization model obtained from the preceding step is utilized to perform the prediction. The optimal parameter combination for SVM is obtained as an outcome of applying GWO algorithm. Then, the resulting parameter combination is set as the optimal parameter of SVM, and the test data is predicted.

1. K-fold cross-validation is performed to split the data set into training set and testing set.

2. Define and set the initial GWO input parameters, comprising the population size, the maximum number of iterations, the upper and the lower bounds of the search space and other algorithm parameters.
3. The a, A, C are initialized by a=2, Eqs. (17) and (18).
4. The grey wolf's position is allocated to the SVM parameter combination (C, σ), and the SVM is trained using the training set and compute the fitness of each grey wolf.
5. Three grey wolves having the maximum fitness are chosen and saved as α, β and δ, the current grey wolf's position is updated according to the best wolf's position as Eqs. (19) – (21).
6. The parameter combination (C, σ) of SVM is set as the updated grey wolf's position.
7. Update α, β and δ, update to reduce the value of a from 2 to 0 in a linear manner, and then update A and C by Eqs. (12) and (13).
8. Determine if the maximum number of iterations is reached. If YES, then yield $\boldsymbol{\alpha}$ position as the optimal SVM parameter combination $X_{\alpha}(C,\sigma)$. If NO, then jump to step 5 in next iteration.

V. RESULTS & DISCUSSIONS

A. HKPU Database

The HKPU (Hong Kong Polytechnic University) database [35] contains 6,264 images acquired from 156 subjects. Index and middle fingers of each hand has six image samples each, which are acquired from each subject. Hence, each subject delivered 24 images. All images are in bmp format of 580*380-pixel size.

1) Hybrid LPQ-LDP Feature Extraction Results:

An integrated feature vector to train SVM is prepared using Hybrid LPQ-LDP feature extraction.

LPQ results in 256-dimensional feature vector and LDP results in 186-dimensional feature vector. An enhanced histogram is obtained by combining the features of both the techniques based on the mean values of the corresponding histograms. The results of Hybrid LPQ-LDP feature extraction for **HKPU Database** are as shown in Fig. 12:

The comparison of accuracy of existing and proposed approach for HKPU database is as shown.

2) Performance Evaluation Metrics:

The proposed approach is analyzed based on the following parameters:

a) **False Acceptance Rate (FAR):** Percentage of imposters accepted= Imposter scores exceeding threshold / Total Imposter scores: **FP/ (FP + TN)**
b) **False Rejection Rate (FRR):** Percentage of genuine users rejected= Genuine scores exceeding threshold / Total Genuine scores: **FN/ (TP+FN)**
c) **Accuracy=** No. of genuine (correct) samples / Total no. of samples **= 100 - (FAR+FRR)**
d) **Equal Error Rate (EER):** The error rate at which False Acceptance Rate (FAR) and False Rejection Rate (FRR) are equal.

3) Verification

A probe image is selected from the HKPU database for verification. On clicking '**Classification**', the image is classified as either GENUINE or IMPOSTER. As in this case, the selected image for verification is classified as GENUINE.

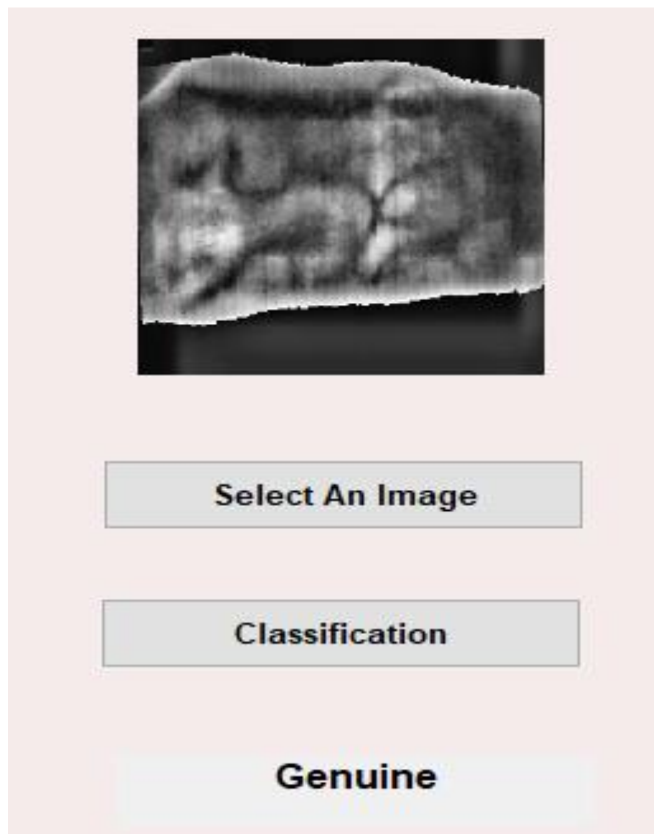

Figure 11. Verification of finger vein image

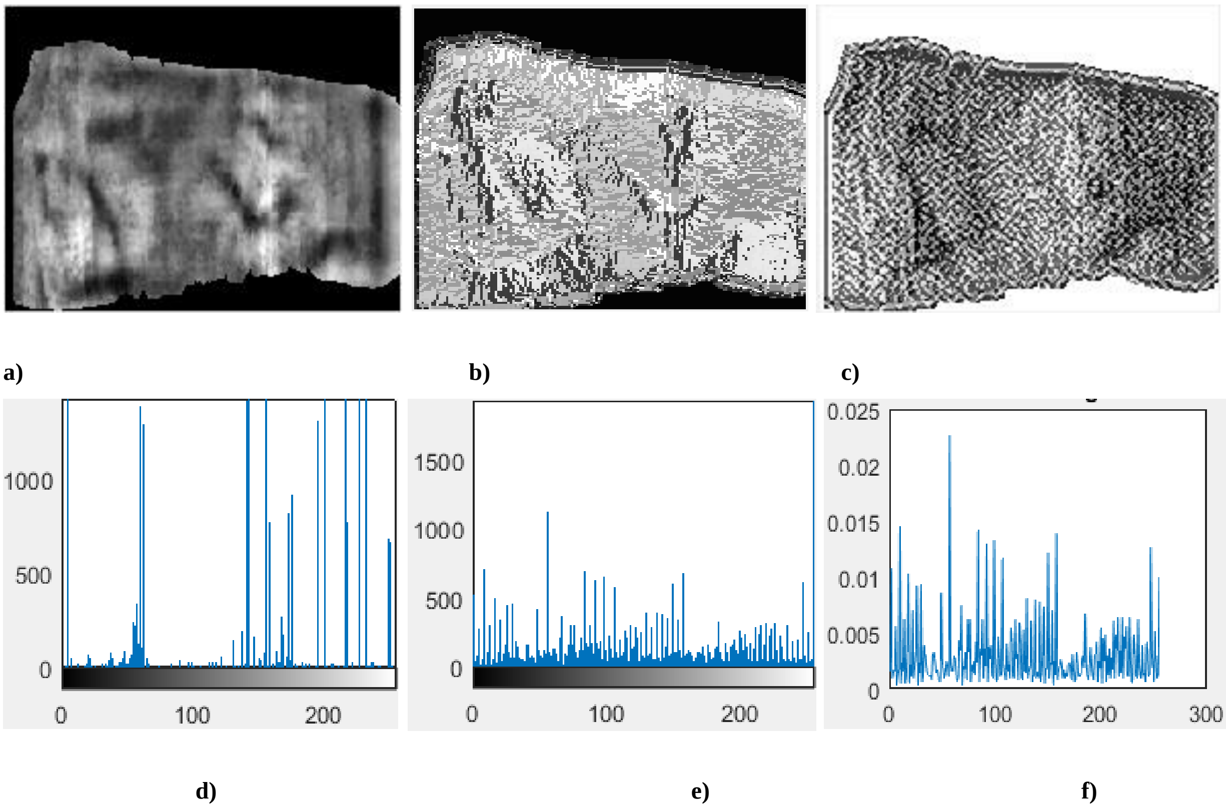

Figure 12. Sample finger vein image feature extraction for HKPU database. a) ROI image of finger vein. b) LDP image. c) LPQ image. d) LDP histogram e) LPQ histogram f) Combined Histogram

4) Comparative Analysis:

Hybrid LPQ-LDP feature extraction proves to be a more robust and efficient technique for finger vein recognition. The proposed GWO-SVM approach has been implemented considering the HKPU finger vein dataset to maximize the classification accuracy by setting the optimal parameter values as shown in Figure 13 and 14. It is observed that the accuracy achieved by typical SVM approach with radial basis function (RBF) kernel without GWO optimization is low and equals to 91.84%, while it achieved an accuracy of 98% using GWO-SVM optimization approach. Hence, it is found that GWO-SVM has performed significantly better than the typical SVM approach and the previous approach (kNCN-SRC) and is more efficient.

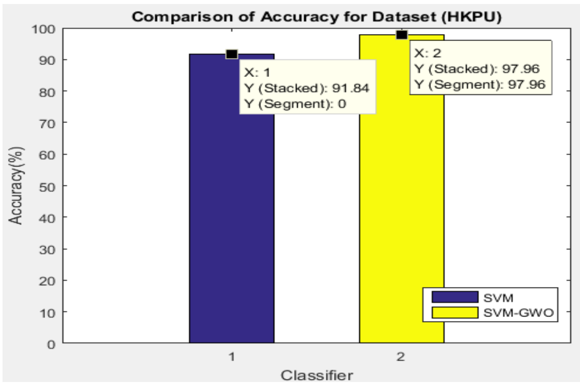

Figure 13. Comparison of SVM and GWO-SVM based on accuracy for HKPU database

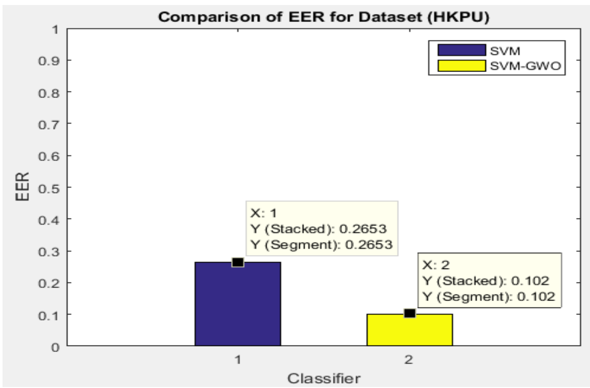

Figure 14. Comparison of SVM and GWO-SVM based on EER for HKPU database

5) Grey Wolf Optimization results

GWO accuracy/fitness based on population size and no. of iterations are as shown in Table 1 and through the five cases:

Case I: Initial population size= 5, Maximum iterations = 15. The plot of GWO fitness vs iteration for population size=5 and maximum iterations=15 is as shown in Fig. 15. It is observed that fitness increases with increasing number of iterations.

Case II: Initial population size= 6, Maximum iterations = 15. The plot of GWO fitness vs iteration for population size= 6 and maximum iterations=15 is as shown in Fig. 16.

Table 1. *GWO fitness (%) based on population size and no. of iterations*

Population Size	No. of iterations		
	5	10	15
5	*83.98 %*	*94.67 %*	*97.96 %*
6	*84.98 %*	*94.34 %*	*97.96 %*
7	*85.57 %*	*95.87 %*	*97.96 %*
8	*90.46 %*	*96.83 %*	*97.96 %*
9	*94.67 %*	*97.96 %*	*97.96 %*

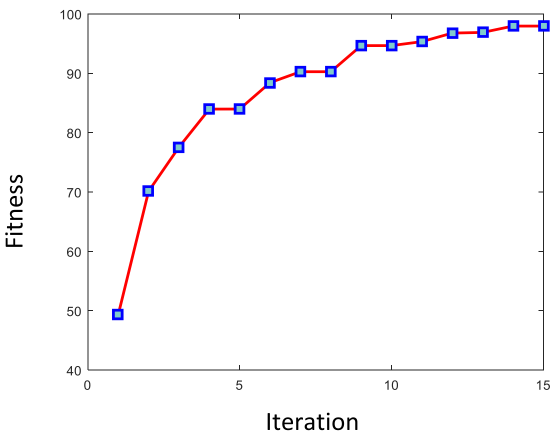

Figure 15. Plot of Fitness vs Iteration: PopSize=5, Maxiter=15

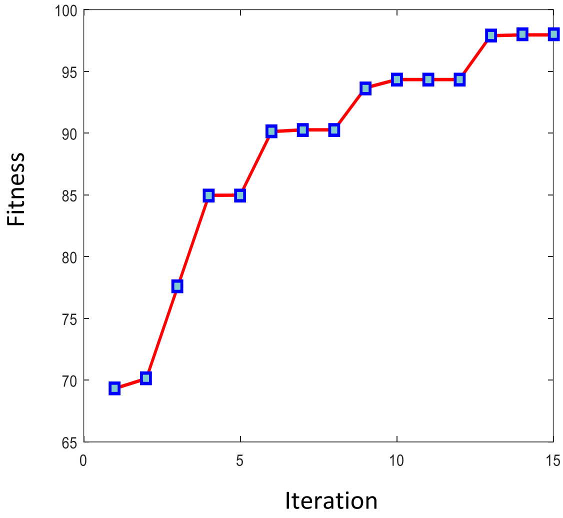

Figure 16. Plot of Fitness vs Iteration: PopSize=6, Maxite

B. FV-USM Database

Finger Vein Universiti Sains Malaysia (FV-USM) Database [33] provided the finger vein images from 123 subjects. Four fingers were provided by every person: left index, left middle, right index and right middle finger in two sittings with an interval of two weeks, with a total of 492 finger classes. Thereby, a total of 5,904 images from 492 finger classes were obtained. The images were resized to a resolution of 30 * 10 pixels.

The LDP, LPQ extracted image, their corresponding histograms and the mean histogram for two finger vein image samples are provided. The results of Hybrid LPQ-LDP feature extraction for **FV-USM Database** are as shown in Fig. 17:

The plot of GWO fitness vs iteration for maximum iterations= 15 for FV-USM is as shown in Fig. 18.

The GWO-SVM achieved an accuracy of 96.94% & EER=0.11 while SVM achieved 95.92% is as shown in Fig.21. The comparison of existing (94%) and proposed approach (96.94%) for FV-USM is as shown in Fig. 19 and

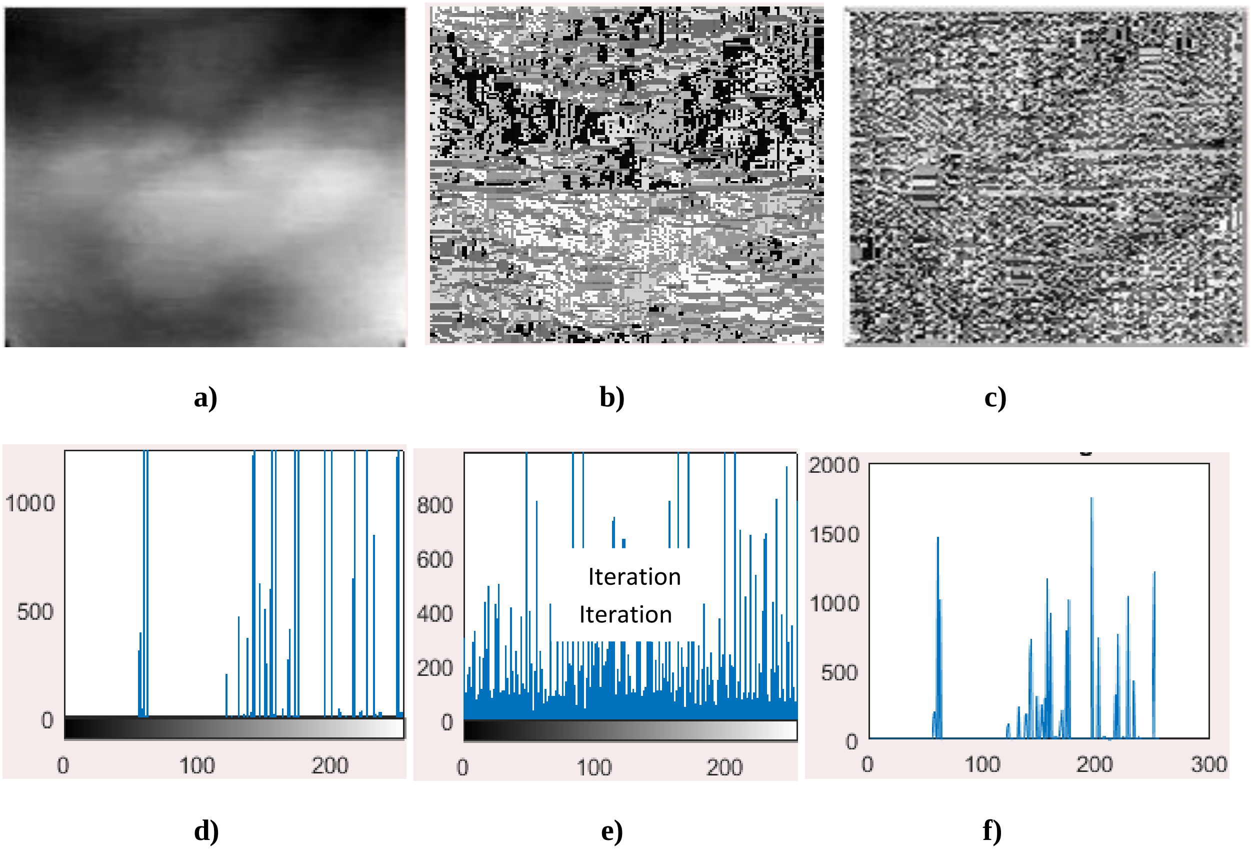

Figure 17. **Sample finger vein image feature extraction for. FV-USM database: a) ROI image of finger vein. b) LDP image. c) LPQ image. d) LDP histogram e) LPQ histogram f) Combined Histogram**

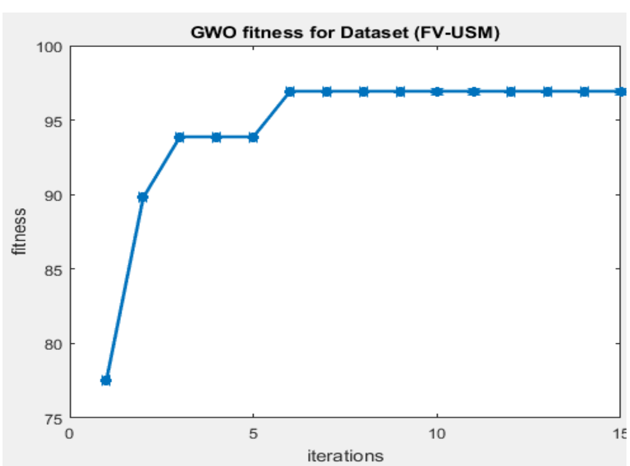

Figure 18. Plot of fitness vs iteration for FV-USM database

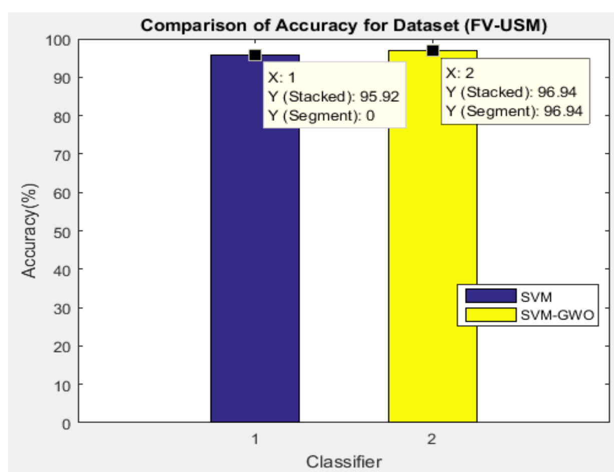

Figure 19. Comparison of SVM and GWO-SVM based on accuracy for FV-USM database

VI. CONCLUSION

Being an intrinsic trait, preferred and highly secure biometric approach, Finger Vein Recognition has been explored in my work. It has a numerous applications such as ATM, internet banking, corpse identification, criminal inspection/analysis to enable a very high security authentication. The accuracy of the personal recognition system is the most severe issue to reflect on. LPQ-LDP extraction is employed which uses directional as well as phase information instead of magnitude information to overcome existing challenges in finger vein recognition. A more accurate and clear feature vector has been obtained using LPQ-LDP feature extraction.

Furthermore, a Grey Wolf Optimization based hybrid Support Vector Machine (GWO-SVM) has been proposed to achieve more efficient and optimal results. The SVM's accuracy highly depends upon the soft margin parameter (C) and kernel function parameter sigma (σ). Thus, the pair (C, σ) is required to be optimized to augment the accuracy of SVM. The experimental results are analyzed based on four parameters, namely, Accuracy, Equal Error Rate (EER), False Acceptance Rate (FAR) and False Rejection Rate (FRR). Our proposed approach demonstrates more robust, efficient and satisfactory results with high accuracy on both datasets outperforming existing techniques.

In future, multiple fingers such as index, middle and ring finger can be authenticated simultaneously using this optimized framework, henceforth the fusion of more than one finger can enhance both security and performance. The multimodal biometric system can also be explored by combining finger vein, finger knuckle and fingerprint features for a more secure user authentication.

REFERENCES

[1]. N. Miura, A. Nagasaka, T. Miyatake, "Extraction of Finger-Vein Patterns Using Maximum Curvature Points in Image Profiles", IAPR Conference on Machine Vision Applications, Vol. E90-D, Issue 8, 2007, pp. 1185-1194.

[2]. K. Shaheed, H. Liu, G. Yang, I. Qureshi, J. Gou, Y. Yin, "A Systematic Review of Finger Vein Recognition Techniques", Information 2018, Vol. *9*, pp. 213.

[3]. V. Ojansivu and J. Heikkil¨a, "Blur Insensitive Texture Classification using Local Phase Quantization," Image and Signal Processing, pp. 236–243, 2008.

[4]. T. Jabid, M. H. Kabir, and O. S. Chae, "Local Directional Pattern (LDP) for Face Recognition," IEEE International Conference on Consumer Electronics, January 2010.

[5]. Mirjalili, S., Mirjalili, S.M., Lewis, A, "Grey wolf optimizer". Adv. Eng. Soft. 69, pp. 46–61, 2014.

[6]. N. Cardoso et.al, "Finger Vein Recognition Using Gabor Filter and Support Vector Machine", IEEE IPAS'14: International Image Processing Applications AND Systems Conference, 2014.

[7]. Yu Lu, "Pyramid Histogram of Double Competitive Pattern for Finger Vein Recognition", IEEE Access, vol.6, pp. 56445-56456, 2018.

[8]. R. Das, E. Piciucco, E. Maiorana and P. Campisi, "Convolutional Neural Network for Finger-Vein-based Biometric Identification," IEEE Transactions on Information Forensics and Security, vol. 14 , issue. 2, 2018, pp. 360 – 373.

[9]. C. Hsia, "New Verification Strategy for Finger-Vein Recognition System," IEEE Sensors Journal, vol. 18, issue. 2, 2018, pp. 790 – 797.

[10]. X. Meng, X. Xi, G. Yang and Y. Yin, "Finger vein recognition based on deformation information," Science China Information Sciences, Springer, 2017.

[11]. Shazeeda, B. A. Rosdi, "Nearest Centroid Neighbor Based Sparse Representation Classification for Finger Vein Recognition", IEEE Access, vol. 7, pp. 5874-5885, 2018.

[12]. H. Changlong L. Zuojin, C. Liukui, J. Peng, "Identification of Finger Vein using Neural Network Recognition Research Based on PCA", IEEE 16th International Conference on Cognitive Informatics & Cognitive Computing, pp. 456-460, 2017.

[13]. L. Yang, G. Yang, Y. Yin "Finger Vein Recognition with Anatomy Structure Analysis," IEEE Transactions on Circuits and Systems for Video Technology, vol. 28, no. 8, 2017, pp. 1892 - 1905.

[14]. S. Veluchamy, L.R. Karlmarx, "System for multimodal biometric recognition based on finger knuckle and finger vein using feature-level fusion and k-support vector machine classifier", IET Biometrics, Vol. 6, Issue. 3, pp. 232-242, 2017.

[15]. Fateme Saadat, "A GSA-based method in human identification using finger vein patterns", IEEE 1st Conference on Swarm Intelligence and Evolutionary Computation (CSIEC), 2016.

[16]. P. Kalaimathi, "Extraction and Authentication of Biometric Finger Vein using Gradient Boosted Feature Algorithm", International Conference on Communication and Signal Processing, pp. 723-726, 2016.

[17]. Shazeeda, B.A. Rosdi, "Finger Vein Identification based on the Fusion of Nearest Neighbor and Sparse Representation based Classifiers", Indian Journal of Science and Technology**,** Vol 9(48), 2016.

[18]. M. A. Syarif, T. S. Ong, A. B. J. Teoh and Connie Tee1, "Enhanced maximum curvature descriptors for finger vein verification", Multimedia Tools and Applications, Vol. 76, No. 5, 2016, pp. 6859–6887.

[19]. B. A. Rosdi, H. Jaafar, and D. A. Ramli, "Finger Vein Identification using Fuzzy-based k-Nearest Centroid Neighbor Classifier", the 2nd ISM International Statistical Conference, pp. 649-654, 2015.

[20]. X. Xiaoming, L. Yang Y. Yin, "Learning Discriminative Binary Codes for Finger Vein Recognition", Pattern Recognition, Elsevier, 2016.

[21]. S. Khellat-kihel, R. Abrishambaf, N. Cardoso, J. Monteiro, M. Benyettou, "Finger Vein Recognition Using Gabor Filter and Support Vector Machine", IEEE International Conference on Image Processing Applications and Systems, 2014.

[22]. G. Yang, X. Xi and Y. Yin, "Finger Vein Recognition Based on a Personalized Best Bit Map", Sensors, Vol. 12, 2012, pp. 1738-1757.

[23]. L. Zhou, G. Yang, Y. Yin, L. Yang and K. Wang, "Finger Vein Recognition Based on Stable and Discriminative Superpixels," International Journal of Pattern Recognition and Artificial Intelligence, vol. 30, no. 6, 2016.

[24]. S. Shazeeda, B. A. Rosdi, "Finger Vein recognition using Mutual Sparse Representation Classification", IET Biometrics, pp. 1-11, 2018.

[25]. S. J. Xie, S. Yoon, J. Yang, Y. Lu, D. S. Park, B. Zhou, "Feature Component-Based Extreme Learning Machines for Finger Vein Recognition", Cognitive Computing, Springer, 2014.

[26]. J. Wu, C. Liu, "Finger-vein pattern identification using principal component analysis and the neural network technique", Expert Systems with Applications, Elsevier, 38, pp. 5423–5427, 2011.

[27]. J. Wu, C. Liu, "Finger-vein pattern identification using SVM and the neural network technique", Expert Systems with Applications, Elsevier, 38, pp. 14284–14289, 2011.

[28]. C. Liu, Y. H. Kim, "An Efficient Finger Vein Extraction Algorithm Based on Random Forest Regression with Efficient Local Binary Patterns", IEEE ICIP, pp. 3141-3145, 2016.

[29]. Zhao, Guoying, and Matti Pietikainen. "Dynamic texture recognition using local binary patterns with an application to facial expressions", IEEE Transactions on Pattern Analysis and Machine Intelligence 29.6 pp. 915-928, 2007.

[30]. Jang, J.-S.R., "ANFIS: adaptive-network-based fuzzy inference system", IEEE Transactions on Systems, Man and Cybernetics. 23 (3): pp. 665–685. 1993.

[31]. X.-S. Yang; S. Deb, "Cuckoo search via Lévy flights", World Congress on Nature & Biologically Inspired Computing (NaBIC 2009). IEEE Publications. pp. 210–214, 2009.

[32]. I. Fister, X. Yang and J. Brest, "A Comprehensive Review of Firefly Algorithms," Swarm and Evolutionary Computation, vol. 13, pp. 34-46, 2013.

[33]. M. S. M. Asaari, S. A. Suandi, and B. A. Rosdi, "Fusion of band limited phase only correlation and width centroid contour distance for finger based biometrics," Expert Syst. Appl., vol. 41, no. 7, pp. 3367_3382, Jun. 2014.

[34]. Y. Yin, L. Liu, and X. Sun, `"SDUMLA-HMT: A multimodal biometric database," in Proc. 6th Chin. Conf. Biometric Recognit. Biometric Recognit., Dec. 2011, pp. 260_268.

[35]. A. Kumar and Y. Zhou, "Human identification using finger images," IEEE Trans. Image Process., vol. 21, no. 4, pp. 2228_2244, Apr. 2012.

[36]. W. Yang, F. Zhou, and Q. Liao, "Feature-level fusion of finger veins and finger dorsal texture for personal authentication based on orientation selection,"' IEICE Trans. Inf. Syst., vol. 97, no. 5, pp. 1371-1373, May 2014.

[37]. E. Piciucco, E. Maiorana and P. Campisi, "Palm vein recognition using a high dynamic range approach", IET Biometrics, Vol. 7, No. 5, 2018, pp. 439 - 446.